Mathematical Modelling, Vol. 3, pp. 279–291, 1982
Printed in the USA. All rights reserved.

0270-0255/82/040279-13$03.00/0
Copyright © 1982 Pergamon Press Ltd.

A MODEL OF THERMALLY INDUCED STRAIN DEVELOPMENT IN COKE OVEN WALLS DURING CARBONIZATION

V. R. VOLLER AND M. CROSS

Mineral Resources Research Center
University of Minnesota
Minneapolis, Minnesota 55455

Communicated by X. J. R. Avula

Abstract—During the carbonization of coal, the thermal conditions within the supporting coke oven walls vary substantially. This gives rise to a continually developing strain field within the walls which could cause cracks to occur in the refractory materials and, thus, shorten the operating life of the oven. Since a more precise knowledge of the location of high strain regions should help in improving the design of coke ovens, a mathematical study was initiated to identify the conditions under which high strain gradients are induced during carbonization. As such, this paper outlines the construction and application of a mathematical model to evaluate the strain distribution and its development in coke oven walls during carbonization. The model includes the influence of all the main thermal and physical properties of silica refractory bricks within a finite element formulation to evaluate the temperature and thermally induced strain distributions in a cross-section of a coke oven wall. The thermal strain field for a typical oven design is calculated at a number of stages throughout the carbonization cycle. The model results provide a clear picture of the nature of the thermal strain distribution and its development, highlighting three areas where the strain conditions in the wall will be most severe.

1. INTRODUCTION

The coking process has long served the needs of the industrial world by providing a relatively efficient reductant of the ferrous oxides. This traditional process has evolved to its current technological state largely through the lessons learned in operational experience.

Today, all metallurgical coke is made in vertical "slot-type" ovens; long, narrow silica brick chambers which are heated indirectly by the combustion of fuel gas in vertical flues. The largest of these ovens are about 14 m long, 6.5 m deep, and 0.45 m wide. To conserve both heat and space, coke ovens are built in batteries consisting of between 10–100 separate ovens, with the heating flues built into the walls which separate the ovens. Carbonization takes 12 to 18 h depending on the width of the oven and the temperature of the flue walls. When coking is complete, the doors on the ends of the oven are removed and the coke charge pushed out. As soon as the charge is cleared, the doors are replaced and then sealed, so that the oven is ready for recharging.

Enough coal for one oven charge is contained in a larry car mounted on rails which run along the top of the oven battery. When an oven is ready for charging, the larry car

This paper was presented at the 3rd International Conference on Mathematical Modelling at the University of Southern California, Los Angeles, July 29–31, 1981.

is positioned and the coal dropped into holes along the top length of the oven. Immediately before charging, the oven side of the flue wall will be at or near to the temperature in the flue. On charging, the coal which is at ambient temperature will rapidly cool the oven side of the wall. Hence, there will be a large temperature gradient across the wall which will diminish as carbonization proceeds.

The changing thermal conditions in the coke oven walls during carbonization will lead to a developing field of strain. This in turn may cause certain areas in the refractory brick wall to crack thereby leading to a shorter operating life for the coke oven.

The purpose of the current work was to develop a model to examine the strain distribution and development in the walls of a coke oven during carbonization, in order to identify the areas with large strain gradients, where the oven walls will be most prone to failure. The modelling programme was carried out in two parts:

(i) the modelling of the thermal properties of the silica bricks, which make up the coke oven refractory walls, and

(ii) application of a finite element model, to determine the temperature and strain distributions in the walls.

2. MODEL DEVELOPMENT

After the study of the designs of coke ovens in general use [1] the dimensions of a "model" oven were chosen. This oven is illustrated in Fig. 1 by a quarter plan view.

2.1. *Assumptions for the model oven*

Before the above modelling programme can be effectively carried out, some simplifying assumptions have to be made:

(i) the coke oven walls and doors are constructed in silica brick;
(ii) only a quarter cross-section (a slice) of the oven is considered under the constraint of plane strain;
(iii) the silica brick behaves in an elastic fashion during the coking;
(iv) on charging, the walls and the doors are at a uniform temperature;
(v) the coke wall interface is at a uniform temperature at any point in time;
(vi) the width of the oven is constant.

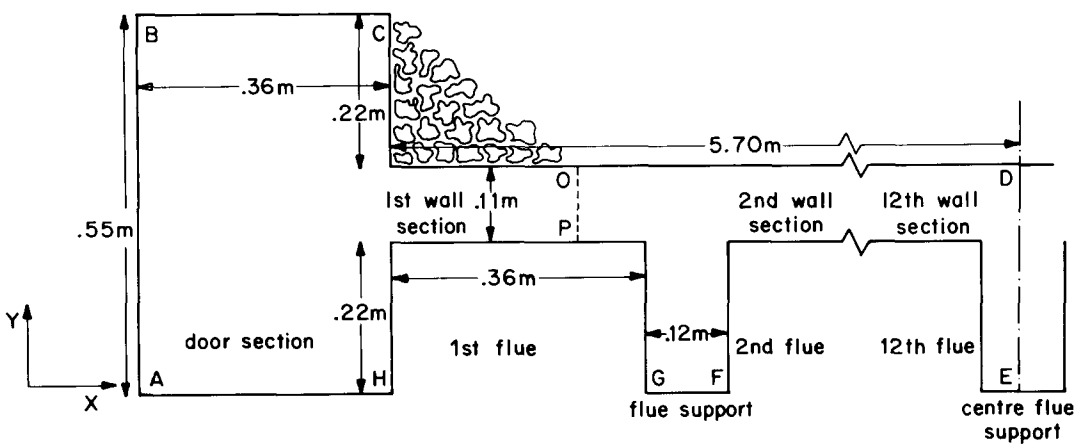

Fig. 1. Quarter plane view of coke oven.

These simplifications mean that

(i) the variation of refractory materials used in a coke oven is not accounted for; as the lining on the door is exposed to the atmosphere for fairly long periods and silica brick is prone to cracking when cooled quickly a different refractory material is often used;

(ii) the loading up the height of the oven walls is uniform and end effects have been ignored;

(iii) the effects of plasticity are ignored [2], however, such effects do not become important until 1200 °C which is at the top of the operating range of a coke oven;

(iv) any heat lost from the door when open, during the pushing of the coke charge, is regained before the oven is charged again;

(v) no account of the temperature variations down the length and height of the wall/coke interface has been taken;

(vi) no allowance has been made for the tapering between the coke oven walls to make the pushing of the coke easier.

Even with these simplifications it should still be possible to identify the areas with high strain gradients and in this work it is the positioning and nature of these areas which is important. Cross *et al.* [2] used similar assumptions in looking at strain generation during the firing of silica shapes, and the predictions for the areas of failure agreed with coupled experimental work.

2.2. *Modelling the thermal properties of silica brick*

Silica brick consists of approximately 96% silica. The remainder is 2% added lime and 2% impurities. The bricks are made from a mixture of finely crushed quartzite rock commonly known as "ganister," and a binding agent, usually milk of lime. This mix is moulded into shape and burned slowly at high temperatures.

2.2.1. *Thermal expansion.* Silica consists of a mixture of quartz, cristobalite and tridymite with specific gravities 2.65, 2.26, and 2.37, respectively [3]. When a silica brick is first fired the quartz changes into the forms with lower specific gravities. These changes are accompanied by large expansions, for example, any unconverted quartz changes into cristobalite at 573 °C with a thermal expansion of 0.45% [1, 3]. After firing, when the silica brick is cooled the rate of reconversion of the tridymite and cristobalite is very small and it can be assumed that once fired, the quartz that has been converted into cristobalite and tridymite will remain in that form. Therefore, it is desirable to convert as much quartz as possible during firing. To achieve this firing schedules run to the order of 170 h [2]. Typical silica brick for commercial kilns shows 5% unchanged quartz [1]. A plot of the coefficient of thermal expansion against temperature is given by Spiers [3, p. 291]. The variation with temperature of the coefficient of thermal expansion, $\alpha(T)$, is modelled by the following piecewise function

$$\alpha(T)\times 10^6 = \begin{cases} 0.3\times T & T < 167\,^\circ\text{C} \\ 50 & 167\,^\circ\text{C} \le T < 200\,^\circ\text{C} \\ 50 + 0.55(T-200) & 200\,^\circ\text{C} \le T < 250\,^\circ\text{C} \\ 77.5 - 1.15(T-250) & 250\,^\circ\text{C} \le T < 300\,^\circ\text{C} \\ AT^2 + BT + C & 300\,^\circ\text{C} \le T \end{cases} \tag{1}$$

where, if $T \ge 580\,^\circ\text{C}$,

$$A = 0.3393\times 10^{-3} \quad B = -0.3175 \quad C = 84.7143,$$

otherwise,

$$A = 0.54439 \times 10^{-4} \quad B = -0.11148 \quad C = 61.045.$$

2.2.2. *Specific heat.* Mean specific heats between 0 and T °C for some refractory materials, including silica, are tabulated by Spiers [3, p. 171]. The heat content of a unit mass of silica is

$$C_m(T)T = \int_0^T C(\alpha)\,\mathrm{d}\alpha \text{ J}, \tag{2}$$

where C_m is the mean specific heat and C is the true specific heat. Differentiating both sides of Eq. 2 with respect to temperature T and using Leibnitz's rule for the differentiation of an integral, yields

$$C(T) = C_m + \frac{\mathrm{d}C_m}{\mathrm{d}T} T \text{ J/kg K}, \tag{3}$$

so the true specific heats can be tabulated. The specific heat at any specified temperature is then found by a linear interpolation between the two nearest tabulated temperatures.

2.2.3. *Thermal conductivity.* The thermal conductivity $K(T)$ depends on both the porosity of the silica brick and the temperature. Cross *et al.* [2] cite unpublished experimental work which measures the thermal conductivity against porosity for various values of temperature. In this problem, the silica bricks are taken to have a porosity of 25%. With this value the variation of conductivity is linear and the thermal conductivity may be simply modelled by

$$K(T) = 5.8T \times 10^{-4} + 1.044 \quad \text{W/m}. \tag{4}$$

2.2.4. *Density.* The bulk density at any temperature $\rho(T)$ is related to the bulk density at zero ρ_0 via

$$\rho(T) = \rho_0/(1 + \alpha T)^3 \quad \text{kg/m}^3. \tag{5}$$

The bulk density at zero is related to the voids fraction, ϵ, and the specific gravity, ρ_s, by

$$\rho_0 = \rho_s(1 - \epsilon) \times 10^3 \quad \text{kg/m}^3.$$

From above the voids fraction is 0.25 and Spiers [3] gives a range of 2.32–2.35 for the specific gravity of silica brick. Choosing a value of 2.33 for the specific gravity gives $\rho_0 = 1750\ \text{kg/m}^3$, which is in agreement with Spiers.

Equations 1 through 5 model the thermal properties of silica brick required in the finite element model of strain development. The model of strain development also requires the values of Poisson's ratio and Young's modulus. In the analyses presented below these will take the constant values of 0.25 and $1160 \times 10^6\ \text{N/m}^2$, respectively [2].

2.3. *Modelling the strain development*

The model for the strain and temperature distribution in the oven walls is based on finite element techniques. The finite element analysis used in determining the tem-

perature distribution will be a "variational" approach [4], while for the strain distribution the more direct "displacement" approach [4, 5] will be employed. Due to the transient nature of the heat conduction the model is developed using finite elements in the space domain and finite differences in the time domain. Before these finite element techniques can be used the region of interest has to be divided up into a triangular [6] grid.

2.3.1. *The temperature distribution.* Within any cross section of the oven wall, the temperature $T(x, y, t)$ satisfies the two-dimensional Fourier heat conduction equation,

$$\frac{\partial^2 T}{\partial x^2} + \frac{\partial^2 T}{\partial y^2} = \frac{\rho C}{K} \frac{\partial T}{\partial t}, \tag{6}$$

while on the surface S,

$$T(x, y, t) = T_1 \quad \text{on} \quad S1 \tag{7a}$$

$$\frac{\partial T}{\partial n}(x, y, t) = 0 \quad \text{on} \quad S2, \tag{7b}$$

where T_1 is a fixed temperature, $\partial/\partial n$ denotes differentiation along the normal to S, and $S1 + S2 = S$. By defining

$$\theta = \frac{-\rho C}{K} \frac{\partial T}{\partial t},$$

and using variational calculus, the solution of Eq. 6 is equivalent to finding the function $T(x, y, t)$, which minimizes the functional

$$\psi(T) = \int_D \int \left\{ \frac{1}{2} \left[\left(\frac{\partial T}{\partial x} \right)^2 + \left(\frac{\partial T}{\partial y} \right)^2 \right] - \theta T \right\} dx\, dy \tag{8}$$

subject to $T(x, y, t)$ satisfying Eq. 7a.

The temperature within any element may be approximated as a linear function of the element nodal temperatures. The unknowns are then the temperature values at the nodes. Substitution of this temperature approximation in Eq. 8 and subsequent differentiation with respect to temperature leads to a set of nonlinear matrix ordinary differential equations [4],

$$\mathbf{H}\mathbf{T} + \mathbf{C} \frac{\mathrm{d}}{\mathrm{d}t} \mathbf{T} = 0 \tag{9}$$

where $\mathbf{T}$ is a list of the nodal temperatures, $\mathbf{H}$ is a matrix dependent upon the triangulation, and $\mathbf{C}$ is another matrix which depends both on the triangulation and the value $\rho C/K$ within each triangle.

Assuming that $T(x, y, t)$ is linear and ρ, C, and K are constant with respect to time within each time interval, the temperature variation at each of the nodes can be calculated from [2, 7]

$$\mathbf{T}_{j+1} = \left(\frac{2}{3}\mathbf{H} + \frac{1}{\delta t}\mathbf{C} \right)^{-1} \left(\frac{1}{\delta t}\mathbf{C} - \frac{1}{3}\mathbf{H} \right) \mathbf{T}_j, \tag{10}$$

where $\mathbf{T}_j$ and $\mathbf{T}_{j+1}$ are the temperature distribution at times $t = j\delta t$ and $t = (j + 1)\delta t$, respectively.

2.3.2. *The strain distribution.* For the strain analysis, the displacement approach [4, 5] of finite elements is used. This is done by invoking the results for a simple elastic beam and then generalizing to account for the plane surface under consideration. In a simple elastic beam, the displacement is proportional to the applied force and in the finite element method this concept is generalized so that the forces at the nodes define their subsequent displacements, i.e.,

$$\mathbf{F} = \mathbf{K}\mathbf{a}, \tag{11}$$

where **F** lists the nodal forces, **a** lists the corresponding nodal displacements, and K is the "stiffness" matrix [4, 5] dependent upon the triangulation and the material properties. Assuming that the nodal forces are determined solely by the temperature distribution and material expansion characteristics the strain within each element may be determined by the relative displacements of its nodes and its natural (or unconstrained) thermal expansion. The global formulation for the strain distribution across the element mesh can be written as [2, 4]

$$\boldsymbol{\epsilon} = \mathbf{B}\mathbf{a} - (1+\nu)\boldsymbol{\alpha}\mathbf{T}, \tag{12}$$

where ν is the Poisson ratio and $\boldsymbol{\alpha}\mathbf{T}$ represents the natural thermal expansion of each element.

2.3.3. *Software notes.* The computer code used in the finite element analysis was a modified version of an interactive computer package [8, 9], written in BASIC$^+$ for the DEC-RSTS/E time sharing system. This package includes an automatic mesh generator based on a triangulation algorithm devised by Lewis and Robinson [6]. The resulting triangular mesh for the oven wall quarter slice, used in both the heat conduction and strain development submodels is shown in Fig. 2. This figure illustrates the advantage in using a finite element technique; in that areas of interest, in this case around the corners [2] and on the wall/coke interface, can be covered by a finer mesh.

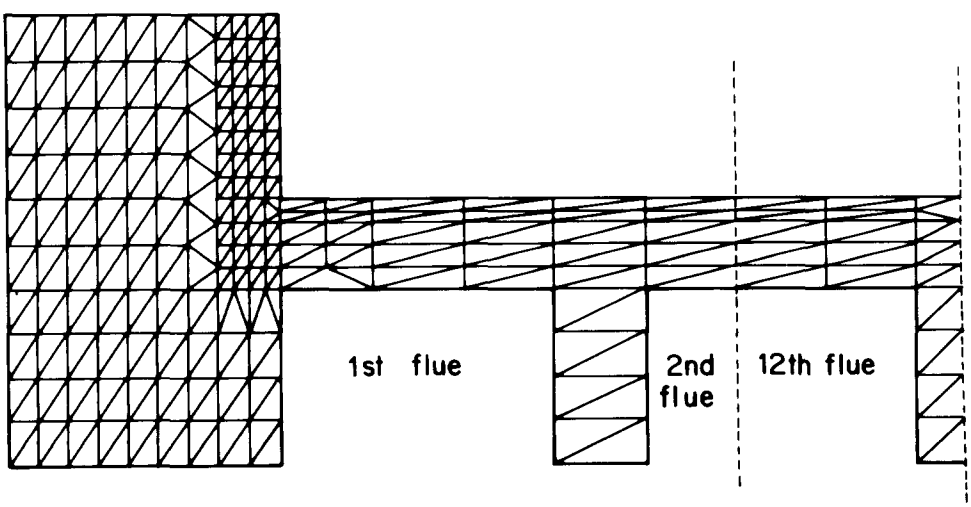

Fig. 2. Triangular mesh used in finite element model: 844 elements, 542 nodes.

2.4. *Implementation of the model*

Time steps of 6 min were used in the model up to 30 min, then time steps of 30 min were used up to 3 h. The smaller time step at the beginning is needed because the strain distribution is changing rapidly due to the large temperature changes in the wall. The model is terminated at 3 h because any temperature changes in the wall after this time are relatively small.

The boundary conditions used for the heat conduction model were as follows. The oven wall was assumed to be perfectly insulated except along the coke/wall interface, $C \leftrightarrow D$ in Fig. 1. Along this interface there is a prescribed temperature, constant at each time step. Values for these temperatures were predicted on use of a coke oven temperature history model developed by Merrick [10–12]. Although the Merrick coke oven model has dimensions and thermal properties differing from the coke oven model of this problem, it was felt that the temperatures listed in Table 1 were depictive for most coke ovens.

The boundary conditions for the strain model were more complex. On reference to Fig. 1, it may be seen that points on symmetry lines are restricted from moving perpendicular to those lines. Clearly this means that the point E in Fig. 1 is fixed. The picture becomes complicated when considering the restrictions for the nodes along the outside of the oven door, $A \leftrightarrow B$ in Fig. 1. During precharge, the outside of the oven door is allowed to expand with no restrictions in the x direction. Immediately before the oven is charged, however, latches drop and the door is prevented from moving in the x direction. Therefore, the software had to be modified to incorporate a time dependent loading on the boundary. At the precharge time step, points between $A \leftrightarrow B$ (Fig. 1) were allowed to move in the x direction. Then at time $t = 0$, i.e., at charging, the loading was changed so those points were fixed in the x direction.

If the quarter slice is taken from the top of the oven, then the above conditions on the boundary nodes are sufficient. The bottom of the coke oven, however, is assumed to be fixed to a rigid concrete base. Therefore, in a slice lower down, the oven movement will be more restricted. The strain development in a lower slice of the coke oven was modelled by fixing the nodes along the "flue-divide" symmetry lines, $G \leftrightarrow F$ in Fig. 1, in addition to the above displacement conditions. To ensure that plane strain approximations could be made, two models needed to be considered; a "top slice" model and a "bottom slice" model. The restriction on the displacement of the boundary nodes for both these models are summarized in Table 2.

Table 1. Temperature of coke/wall interface with time.

Time m	Temperature °C
Precharge	1050
0	100
6	350
12	534
18	715
24	759
30	762
60	799
90	834
120	859
150	878
180	893

Table 2. Summary of boundary conditions for stress/strain model.

Precharge		Postcharge	
Status	Position on Fig. 1	Status	Position on Fig. 1
Top Slice Model			
Fixed in X and Y	$i = E$	Fixed in X and Y	$i = A, i = B,$ $i = E$
Fixed in X	$i \in [D, E[$	Fixed in X	$i \in [D, E[$ $i \in]A, B[$
Fixed in Y	$i \in [H, A]$ $i \in [B, C]$ $i \in [G, F]$	Fixed in Y	$i \in [H, A[$ $i \in]B, C]$ $i \in [G, F]$
Bottom Slice Model			
Fixed in X and Y	$i = E, i = G,$ $i = F$	Fixed in X and Y	$i = E, i = G,$ $i = F, i = A, i = B$
Fixed in X only	$i \in [D, E[$	Fixed in X and Y	$i \in [D, E[$ $i \in]A, B[$
Fixed in Y only	$i \in [H, A]$ $i \in [B, C]$	Fixed in Y only	$i \in [H, A[$ $i \in]B, C]$

Key: $]A, B[$ all points between A and B excluding A and B; $[A, B]$ all points between A and B including A and B; $[A, B[$ all points between A and B including A excluding B.

Note that a number of meshes and a combination of time steps were tried and tested for stability before the mesh given in Fig. 2 and the time steps given above were chosen.

3. RESULTS AND DISCUSSION

3.1. *Areas of interest*

The object of this work is to gain an understanding of the nature of the stress and strain conditions in the coke oven walls during the carbonization process. This can best be done by identifying

(i) areas with large strain concentrations (i.e., areas with high strain gradients) and
(ii) areas where large tensile strains occur.

In these areas the strain conditions in the coke oven walls are at their most severe.

When the nature and distribution of the strain is known at any time, in a cross section of the oven, areas with large tensile strains and large strain concentrations are easily identified. The strain distribution may be determined by drawing a principal strain contour diagram.

For the coke oven wall problem the strain distributions in both the "top" and "bottom" slice models were found at the following specified "investigation" times, t:

(i) $t < 0$ (precharge),
(ii) $t = 0$ (charge),
(iii) $t = 6$ min (postcharge),
(iv) $t = 30$ min (early carbonization),
(v) $t = 3$ h (late carbonization).

In practice, charging the oven takes 1.5–2 min and so the charge time $t = 0$ represents an approximation. The investigation times were chosen to determine the strain distribution in the oven:

(i) in the relaxed state, i.e., when all points are at a constant temperature (1050 °C) and the door can expand freely in the x direction;
(ii) during charging, when the largest strain concentrations should occur;
(iii) when the strain development is rapid;
(iv) as the rate of change in temperature on the wall/coke interface slows and
(v) as the strain development ceases.

The results for the five chosen investigation times, t, are discussed below. Due to space considerations only the strain distribution in the oven door section and the first three flue supports will be illustrated. In fact, apart from the central flue support where small tensile strains occur, the strain pattern in the wall sections and flue supports remains unchanged after the third flue support. An additional saving of space will be made by only illustrating the strain distributions in the bottom slice where the largest strain concentrations occur. (Note that throughout the discussion the corners where the wall joins the door section are referred to as the wall/door corners).

3.2. *Precharge* $t < 0$

The strain distribution in a bottom slice is shown in Fig. 3. There are large strain concentrations at the wall/door corners. Strain concentrations at corners are normal in this type of problem (see Cross *et al.* [2]). There are small tensile strains in the first wall section but these are not considered important. There are however, large tensile strains and a high strain gradient in the flue divides near the door. In flue divides near the center of the oven wall, the tensile strains vanish but high strain gradients are still in evidence at the divide bottoms, i.e., along the symmetry lines $F \leftrightarrow G$ in Fig. 1. The strain distributions in the flue divides are due to the bottom of the divides being fixed at lower cross-sections in the oven. This results in the tops of the flue divides being bent towards the door as expansion takes place in the x direction. In fact, the strain distribution in the first divide resembles that found in a bent rod. In the flue divides nearer the center of the oven, the bending of the flue divides is much less, hence, the tensile strains disappear. However, this "bending" still causes the strain concentration at the bottom of these divides.

3.3. *Charge* $t = 0$

On charging there is a very steep strain gradient along the coke/wall interface (Fig. 4). This gradient becomes less steep at points near the center of the oven.

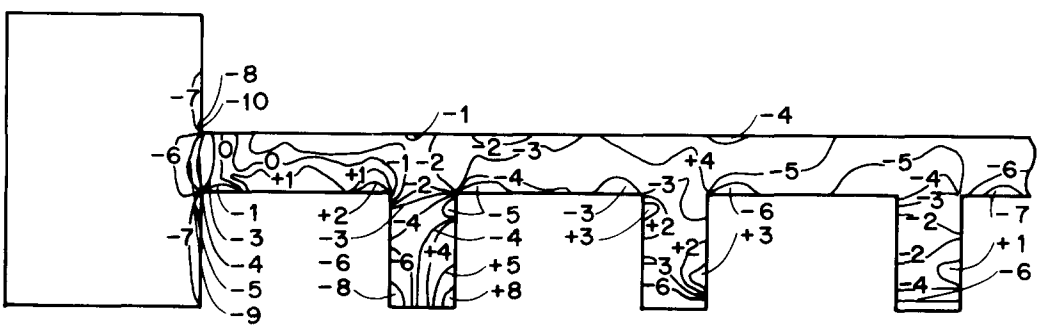

Fig. 3. Strain contours at time $t < 0$: Bottom slice.

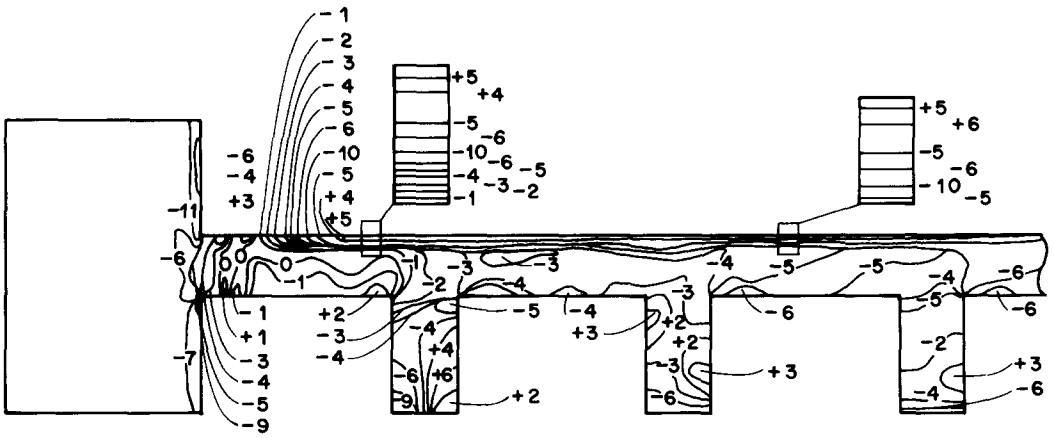

Fig. 4. Strain contours at time $t = 0$: Bottom slice.

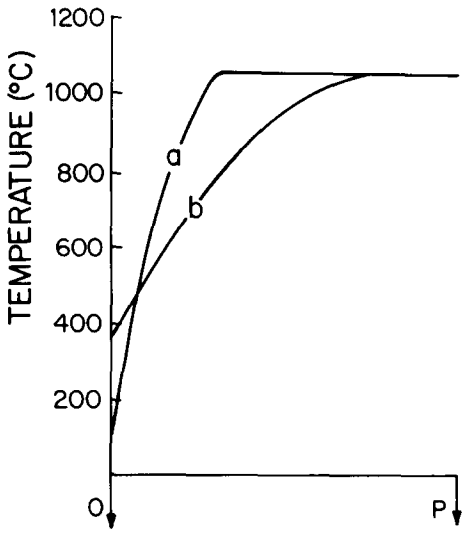

Fig. 5. Temperature gradient across first wall section (points O–P in Fig. 1), at times $t = 0$, curve a, and $t = 6$ min, curve b.

The reason for this large strain concentration at the coke/wall interface can be seen on reference to Fig. 5. Curve a, which indicates a steep temperature gradient at the coke/wall interface, with temperatures in the immediate vicinity of the interface below 600 °C and the temperature in the majority of the wall at 1050 °C. Wilson and Wells [1] note that the thermal expansion of silica only becomes significant at temperatures below 600 °C. Therefore, when charged the part of the oven wall adjacent to the coal will want to undergo a contraction. However this contraction is restricted by the remainder of the wall, which suffers no such thermal dilation. Hence there is a strain buildup at the coke/wall interface.

The conditions in the region of the oven away from the coke/wall interface remain unchanged on charging. This accounts for the strain distribution in those parts of the oven being almost identical to the distribution in the relaxed state.

3.4. *Postcharge t = 6 min*

The strain distribution in a bottom slice of the oven, six minutes after charging, is shown in Fig. 6. The strain concentrations at the coke/wall interface are smaller than at charging. Curve *b* in Fig. 5 shows the temperature gradient across the first wall section at $t = 6$ min. On comparison with the temperature distribution at $t = 0$, curve *a*, it is noticed that the temperature gradient at the wall/coke interface is less steep. This means that thermal contractions are not restricted to the immediate area of the coke/wall interface. This fact accounts for the reduction in the strain concentration along the coke/wall interface.

The strain gradients at the wall/door corners are similar in nature to those at previous time levels. However the gradients are a little steeper than before. In addition, the strain distribution in the flue divides remain unaltered from the relaxed state.

3.5. *Early carbonization t = 30 min*

After 30 min, the strain gradient is fairly uniform across the wall. This is illustrated in Fig. 7, which shows the principal strain contours in a bottom slice. The compressive strain gradient at the wall/door corners is again slightly larger than before. However further results show that this gradient returns to its relaxed state as carbonization continues. As at previous time levels the strain distributions in the flue divides is similar to the relaxed state.

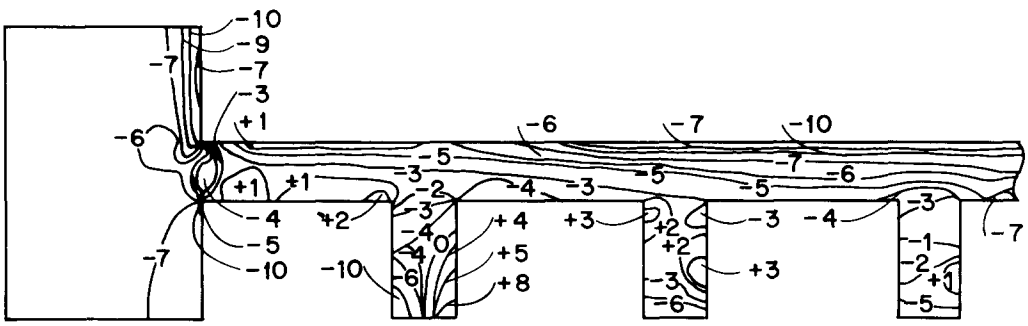

Fig. 6. Strain contours at time $t = 6$ min: Bottom slice.

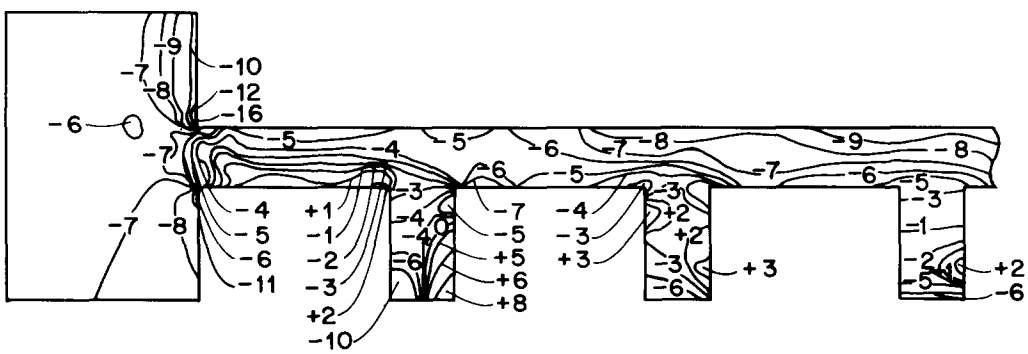

Fig. 7. Strain contours at time $t = 30$ min: Bottom slice.

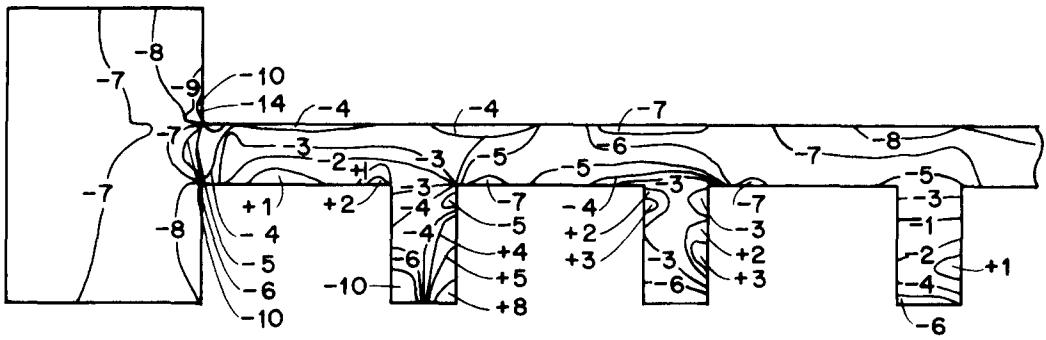

Fig. 8. Strain contours at time $t = 3$ h: Bottom slice.

3.6. *Late carbonization* $t = 3$ *h*

Between thirty minutes and 3 h after charging, the strain distribution appears to develop little. The only significant change in the pattern of the strain distribution during this time takes place in the first wall section. This can be seen by comparing Fig. 8, which shows the strain distribution in a bottom slice three hours after charing, with Fig. 7. Further comparing Figs. 8 and 3, it is noticed that the strain distribution in the oven walls and door 3 h after charging, is similar in nature to that of the relaxed oven. From this, it may be concluded that the strain develops little in the latter stage of carbonization.

3.7. *Summary of results*

The strain distribution and generation in the coke oven walls during carbonization can be summarized as follows:

(i) In the relaxed oven, away from the door, strains in the wall are present in lower cross sections only. These strains are compressive.

(ii) The most marked strain concentration occurs at the wall/coke interface during and just after charging. Included in this strain concentration are areas of tensile strain.

(iii) After thirty minutes of coking the strain concentration at the coke/wall interface has been dissipated and the strain gradient is uniform across the oven wall.

(iv) There is a steep strain gradient at the wall/door corners. This gradient increases over the first thirty minutes of coking and then returns slowly to its precharge value.

(v) The strain distribution in the flue divides alters little during carbonization.

(vi) The largest tensile strains occur in the first flue divides at low cross-sections in the oven.

(vii) The strain distribution develops rapidly over the first thirty minutes of coking.

(viii) The strain distribution develops little during the latter stages of coking.

4. CONCLUSIONS

A model has been developed which gives a clear picture of the strain distribution and development in the walls and door of a coke oven. From the results of this model three areas of the coke oven wall may be identified where the strain conditions are severe

(i) the coke/wall interface during charging,

(ii) the door/wall corners, particularly half an hour after charging, and

(iii) The flue divides at lower cross-sections of the oven, particularly the flue divides near the door.

Finally, in any study of the operational life expectancy of a coke oven, a thermal strain analysis of the type conducted above will be important. However, it should be noted that the thermal expansion and contractions in the oven walls may not be the only strain/stress conditions imposed on the coke oven structure during carbonization. Strain fields in the oven walls caused by the pressure buildup of volatile gases and the expansion of the oven charge may have a significant contribution. The position, magnitude, and nature of such strains is not fully understood, however, and before phenomena of this type can be coupled with the thermal strain model outlined in this paper a number of extensive studies have to be conducted. For example, expansion of the charge needs to be quantified and models of the volatile gas movement [13–15] need to be further developed.

5. REFERENCES

1. P. J. Wilson, and J. H. Wells, *Coal, Coke and Coal Chemicals*, McGraw-Hill, New York (1950).
2. M. Cross, B. A. Lewis, and J. K. Forster, Strain generation during firing of dence silica shapes. *Refract. J.* **1**, 10–22 (1978).
3. H. M. Spiers, Technical data on fuel, Brit. Nat. Com. World Power Conference, 5th Ed. (1950).
4. O. C. Zienkiewicz, *The Finite Element Method*, 3rd Ed., McGraw-Hill, New York (1977).
5. K. H. Hubner, *The Finite Element Method for Engineers*, Wiley, New York (1975).
6. B. A. Lewis and J. S. Robinson, Triangulation of planar regions with applications. *Comp. J.* **21**, 324–332 (1977).
7. B. A. Lewis, Private communication (1978).
8. B. A. Lewis and M. Cross, IFECS – An interactive finite element computing system. *Appl. Math. Modelling* **2**, 165–175 (1978).
9. B. A. Lewis, IFECS—Software for modelling thermal stress problems, in *Modelling and Simulation in Practice*, M. Cross, R. D. Gibson, M. J. O'Carroll, and T. S. Wilkinson, eds., Pentech Press (1979).
10. D. Merrick, Metallurgical coke manufacture: A mathematical study, Ph.D. Thesis, Univ. of London (1977).
11. D. Merrick and B. Atkinson, Coke oven modelling, in *Modelling and Simulation in Practice*, M. Cross, R. D. Gibson, M. J. O'Carroll, and T. S. Wilkinson, eds., Pentech Press (1979).
12. B. Atkinson and D. Merrick, Mathematical models of the thermal decomposition of coal; Part 4, Heat transfer and temperature profiles in a coke oven charge. *Fuel* (in press).
13. G. E. Foxwell, The path of travel of the gases in the coke oven. *J. Soc. Chem. Ind.* **40**, 193T–201T (1921).
14. V. R. Voller, M. Cross, and D. Merrick, Mathematical models of the thermal decomposition of coal; Part 5, The distribution of gas flow in a coke oven charge. *Fuel* (in press).
15. V. R. Voller, A mathematical analysis of some aspects of the coking process, Ph.D. Thesis, CNAA (1980).